Spectral Signature of Low Temperature Hopping Between Two Impurity-Induced Elastic Configurations

R. Lai, C. E. Mungan,* and A. J. Sievers

Laboratory of Atomic and Solid State Physics and Materials Science Center, Cornell University, Ithaca, New York 14853-2501

(Received 20 September 1995)

We demonstrate that the jump-rotational-diffusion model originally developed in the context of quasielastic neutron scattering from high temperature liquids can describe the two-state behavior observed in the low temperature dynamics of some molecular and point defects in crystals. The unusual temperature dependences of the IR spectra of both diatomic chalcogen hydrides in alkali halides and $KI:Ag^+$ can be explained in terms of two elastic configurations between which the impurities jump with temperature-dependent dwell times.

PACS numbers: 63.20.Pw, 33.70.–w, 66.30.Jt, 78.30.Hv

The Debye-Waller-like temperature dependence of the strength of a zero-phonon line is a characteristic signature of coupled electron-phonon dynamics in a wide variety of impurity spectra [1,2]. At the same time, other defect systems have been discovered whose spectral features rapidly disappear with temperature, such as $KI:Ag^+$ [3], $RbCl:Ag^+$ [4], and $KBr:SD^-$ [5], that cannot be understood within this framework. This disappearance is too sudden to be explained in terms of linear defect-phonon coupling or of thermal population of higher-lying energy levels. A systematic investigation of $KI:Ag^+$ has shown that the thermally activated disappearance of the strength of the IR- and Raman-active vibrational modes and the appearance of the UV electronic transitions [3] are associated with the Ag^+ impurity moving from an on-center to an energetically nearby off-center configuration. Stark-effect far-IR measurements and analyses have demonstrated that the on-center configuration is essentially harmonic [6], leaving unanswered the question as to how the second configuration can become dominant over such a restricted temperature interval.

In this Letter, we report temperature-dependent measurements of the IR strengths of the librational modes of diatomic chalcogen hydrides fcc alkali halide crystals. The observed temperature-dependent change in the oscillator strength of these librational modes is well described in terms of a jump-rotational-diffusion model originally developed for neutron scattering work on liquids [7]. This success leads us to propose a more general two-configuration model to encompass point defect systems, such as $KI:Ag^+$. In both cases, the key element of the dynamics is the hopping between elastic configurations, and it is the temperature dependence of this element which determines the rapid temperature dependence of the observed spectral features.

Figure 1(a) shows the vibrational sidebands of the stretching mode of Sd^- in KBr at 1.7, 50, 100, and 150 K obtained from IR absorption measurements. The librational mode appears above the top of the phonon bands at 254 cm^{-1}; notice that its strength disappears without substantial change in its width or center frequency [5]. Analogous measurements on $KBr:SH^-$ show that the 332 cm^{-1} librational sideband mode vanishes by $\sim$150 K in the same manner. Direct far-IR absorption measurements of this latter system reveal a librational mode at 317 cm^{-1} with a similar temperature-dependent strength; in the 2–20 cm^{-1} frequency range, on the other hand, a Debye relaxational spectrum is discovered to *appear* with increasing temperature, coinciding with the disappearance of the librational mode.

Here we adapt the jump-rotational-diffusion model [7–9] so that in one configuration (at low temperatures) the molecules are orientationally confined and only librational motion is possible, while in the other arrangement (at high temperatures) rotational diffusion over a broad range of angles is preferred. The motion of any given dipole is modeled as a stochastic process which is subdivided into successive time steps $0, 1, 2, \ldots, n$. Suppose that the dipole is initially oriented at $t = 0$ with angle $\theta = 0$ and librates for an average time τ_A; next, in time step 1, the dipole jumps to a rotationally diffusive state in which it remains for an average time τ_B; in step 2, it is librating again; and so forth. The self-correlation function, which is the probability of finding the dipole with angle θ at time t, can be written as [7–9]

$$G_s(\theta, t) = \sum_{j=0}^{\infty} F_j(\theta, t), \tag{1}$$

where the function $F_j(\theta, t)$ is defined at each time step according to the description in Ref. [7].

The complex polarizability of a plane rotor $\hat{\alpha}(\omega)$ can be obtained from the two-dimensional Kubo relation [10]

$$\hat{\alpha}(\omega) \equiv \alpha_1(\omega) - i\alpha_2(\omega) = \frac{\mu^2}{2kT}\left[1 - i\omega\int_0^{\infty} dt e^{-i\omega t} c(t)\right], \tag{2}$$

where μ is the permanent dipole moment of the rotor and $c(t)$ is the dipole-dipole autocorrelation function which is related to Eq. (1) by

$$c(t) \equiv \langle \vec{n}(t) \cdot \vec{n}(0) \rangle = \int d\theta \cos\theta G_s(\theta, t) = \int d\theta e^{i\theta} G_s(\theta, t). \tag{3}$$

 0031-9007/96/76(11)/1864(4)$10.00

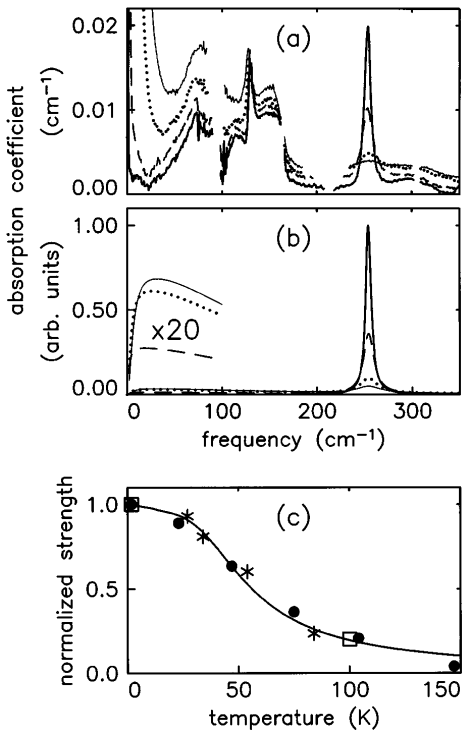

FIG. 1. (a) Vibrational-sideband absorption spectra of ~1400 ppm SD^- in KBr at temperatures of 1.7 K (bold solid curve), 50 K (dashed curve), 100 K (dotted curve), and 150 K (light solid curve). The abscissa gives the frequencies relative to the vibrational mode at ~1866 cm^{-1}; the one-phonon sideband is evident between ~10 and 200 cm^{-1}. (b) Calculated reorientational absorption spectra of KBr:SD^- at the same temperatures as in (a) from Eq. (6) using the parameters given in Table I. The high temperature curves have also been plotted with 20-fold vertical expansion at low frequencies to show the Debye peaks. (c) Integrated absorption strengths (normalized to 0 K) of the experimentally measured librational-sideband modes of KBr:SD^- (filled circles) and KBr:SH^- (open squares), compared to the corresponding theoretically calculated values (solid curve). The asterisks give the rate of increase of the generalized Debye spectrum of KBr:SH^- (measured relative to undoped KBr) in the far infrared, as explained in the text.

Here, $\vec{n}(t)$ is the unit vector along the dipole moment at the time t and the last equality follows from the fact that $G_s(\theta, t)$ is an even function of θ. By taking the Fourier transform of $c(t)$ and substituting the various functions F_j, an infinite series is obtained which reduces to [7]

$$\int_0^\infty dt e^{-i\omega t} c(t) = [\hat{A} + \hat{A}\hat{B}/\tau_A][1 - \hat{A}\hat{B}/(\tau_A\tau_B)]^{-1}, \quad (4)$$

where

$$\hat{J}(\omega) = \int\int d\theta dt e^{i(\theta - \omega t)} p_J(t) g_J(\theta, t), \quad (5)$$

with $J = A$ or B. Here, $g_A(\theta, t)$ and $g_B(\theta, t)$ are the probabilities of finding the dipole at angle θ after a time t if the dipole is in the librational (A) and rotationally diffusive (B) state, respectively, and $p_A(t) = \exp(-t/\tau_A)$ and $p_B(t) = \exp(-t/\tau_B)$ are the corresponding probabilities that it remains in each of these states assuming a Poissonian distribution. Equation (4) is valid if the dipole starts in the librational state. In general, however, the dipole can start in either the librational or rotationally diffusive state, so that $G_s(\theta, t)$ must be averaged over both Eq. (4) and the analogous rotational-diffusion expression (not given) with the respective weight factors $\tau_A/(\tau_A + \tau_B)$ and $\tau_B/(\tau_A + \tau_B)$. Thus one obtains for the complex polarizability

$$\hat{\alpha}(\omega) = \frac{\mu^2}{2kT}\left\{1 - i\omega\left[\frac{\tau_A}{\tau_A + \tau_B}\frac{\hat{A} + \hat{A}\hat{B}/\tau_A}{1 - \hat{A}\hat{B}/(\tau_A\tau_B)} + \frac{\tau_B}{\tau_A + \tau_B}\frac{\hat{B} + \hat{A}\hat{B}/\tau_B}{1 - \hat{A}\hat{B}/(\tau_A\tau_B)}\right]\right\}. \quad (6)$$

Now consider Eq. (6) in two temperature limits. At low temperatures the dipole remains in the librational state ($\tau_A/\tau_B \to \infty$) producing an IR absorption line at the librational frequency, while at high temperatures it spends increasing amounts of time in the rotationally diffusive configuration so that oscillator strength is transferred from the librational mode to a Debye relaxational spectrum. This transfer is controlled by the temperature dependences of the lifetimes τ_A and τ_B, which depend in turn on the geometry of the interaction between the dipole and the lattice. At intermediate temperatures, Eq. (6) demonstrates that the spectral polarizability is determined by an intricate mixture of both states.

We next apply this model to the experimental data for SD^- in KBr. To obtain expressions for $\hat{A}(\omega)$ and $\hat{B}(\omega)$, we treat the librator as a simple Lorentz oscillator and use a generalized Debye spectrum for the rotationally diffusive configuration. One can see from Eq. (5) that the effect of a finite dwell time τ_J ($J = A, B$) is to shift the frequency by an amount $-i/\tau_J$. Evaluating Eq. (6) in the limit $\tau_A \to \infty$ yields

$$\hat{A}(\omega) = \frac{1}{i\tilde{\omega}_A}\left[1 - \frac{kT/I}{\omega_r^2 - \tilde{\omega}_A^2 + i\gamma_A\tilde{\omega}_A}\right], \quad (7)$$

where I is the moment of inertia of the dipole, ω_r is its librational frequency, γ_A specifies the spectral FWHM, and $\tilde{\omega}_A \equiv \omega - i/\tau_A$. Evaluating Eq. (6) for $\tau_B \to \infty$, on the other hand, identifies the rotationally diffusive configuration. Since Debye's original one-pole formula does not conserve oscillator strength, we instead use a two-pole expression which does [10,11]. The result is

$$\hat{B}(\omega) = \frac{1}{i\tilde{\omega}_B}[1 - (1 + i\tilde{\omega}_B\tau_D)^{-1}(1 + i\tilde{\omega}_B\tau_F)^{-1}], \quad (8)$$

where $\tilde{\omega}_B \equiv \omega - i/\tau_B$, τ_D is the Debye relaxation time, and $\tau_F \equiv I/\tau_D kT$ is the friction time.

Although experimentally the strength of the librational mode disappears with increasing temperature, its center frequency does not shift significantly, indicating that the librational potential well is not thermally softened. Clearly, the height of this well is much greater than 150 K, the temperature by which the librational absorption strength has vanished. On the other hand, this disappearance suggests

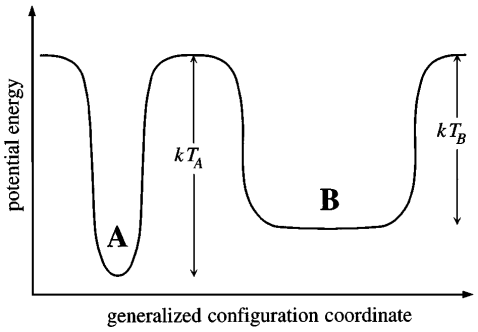

FIG. 2. Schematic potential-energy diagram of the two reorientational states. The librational potential well (A) is deep and narrow, while the rotationally diffusive well (B) is broad and flat bottomed. The energy separation between the two minima is equal to $k(T_A - T_B)$.

that the rotationally diffusive configuration lies ~150 K higher in energy than the librational one. We therefore speculate that the geometry of the potential is something like that sketched in Fig. 2: a deep, narrow, harmonic librational well (A) and a much broader rotationally diffusive well (B). The temperature dependences of the times spent in each configuration are assumed to be given by [12]

$$1/\tau_J = \omega_J \exp(-T_J/T) \quad (J = A, B), \tag{9}$$

where ω_A and ω_B are attempt frequencies of the defect in the different configurations. These frequencies and the barrier heights kT_A and kT_B set the energy scales for the model. Fitted values are given in Table I. Since the librational frequency does not shift with increasing temperature, the librational lifetime τ_A is expected to be much longer than the librational period and hence the linewidth is primarily controlled by the damping constant γ_A. A fit to the measured linewidth of the librational mode gives $\gamma_A = (0.02 + 0.000\,63\,\mathrm{K}^{-1}\,T)\omega_r$. The mm-wave absorption spectrum of KBr:SH^- gives $\tau_D^{-1} = 0.04\,\mathrm{K}^{-1}\,\mathrm{cm}^{-1}\,T$.

With these parameters, the temperature-dependent absorption spectra can be calculated. The results for the impurity-induced absorption coefficient of KBr:SD^-, which is proportional to $\omega\alpha_2(\omega)$, are plotted at various temperatures in Fig. 1(b). With increasing temperature, oscillator strength is transferred from the librational mode to a low-frequency Debye spectrum. While the librational absorption line broadens and vanishes with increasing temperature, its center frequency remains essentially unchanged, reproducing the experimental data in Fig. 1(a).

The strength of the librational mode at each temperature can be found by integrating the background-subtracted absorption spectra over a bandwidth larger than the libron, say 210–290 cm^{-1}. The resulting experimental strengths are plotted as the filled circles in Fig. 1(c), while the solid curve gives the corresponding theoretical results. The two agree with each other to within the experimental uncertainties. The open squares give the experimental strengths of the librational sideband of KBr:SH^-; these data agree with those of KBr:SD^-, indicating that the temperature-dependent effect is not isotope dependent. Finally, the asterisk symbols in this same panel give the rate of increase $[S(\infty) - S(T)]/S(\infty)$ of the absorption strength S of the KBr:SH^- Debye spectrum integrated from 4 to 6.5 cm^{-1}. (At higher frequencies, KBr phonon difference-band absorption masks the Debye spectrum.) It is evident that the Debye strength grows at the same rate as the librational strength vanishes, which strongly supports the model developed above.

This thermally activated disappearance of the strength of the librational modes of the diatomic chalcogen hydrides in fcc alkali halides is reminiscent of the temperature dependence of the defect modes of KI:Ag^+. Previous measurements of this latter system led to the conjecture that two kinds of elastic configurations coexist: an on-center and an off-center one [13]. The dynamics of Ar^+ can be analyzed in terms of two configurations conceptually similar to those described above (cf. Fig. 2): an on-center state (A) in which the Ag^+ atom oscillates harmonically about the lattice site during an average time τ_A, and an off-center configuration (B) in which the ion rotates diffusively about the lattice site during an average time τ_B.

The total far-IR polarizability is then given by Eq. (6), where the functions $\hat{A}(\omega)$ and $\hat{B}(\omega)$ have the same forms as Eqs. (7) and (8), with ω_r now identified with the resonant mode frequency and I replaced by $M\mu^2/e^2$ (e is the electron charge and M is the oscillator mass which we approximate by the Ag^+ ion mass) [14]. The fitted values for the attempt frequencies and barrier heights are listed in Table I. The resulting energy separation of the on- and off-center configurations is therefore 26 K. From rf measurements of the Debye spectrum [15], the measured relaxation time $\tau_D^{-1} = 3 \times 10^{10}\,\mathrm{K}^{-1}\,\mathrm{s}^{-1}\,T$ gives the friction time $\tau_F \equiv I/\tau_D kT$, where the moment of inertia I can be obtained from the measured dipole moment $\mu = 1.5$ D. Since at low temperature ($T < 10$ K) the average dwell time in the on-center state is much longer than the vibrational period, we set the damping constant γ_A equal to the linewidth of the resonant mode as measured in Ref. [16].

TABLE I. Energy scales for the two elastic configurations: ω_r is either the librational frequency of the hydride molecule or the resonant mode frequency of the Ag^+ ion, as appropriate; ω_A is identified with the Debye frequency of the host; ω_B is the attempt frequency in the rotationally diffusive configuration; and T_A and T_B specify the barrier heights in Fig. 2.

	ω_r (cm^{-1})	ω_A (cm^{-1})	ω_B (cm^{-1})	T_A (K)	T_B (K)
KBr:SD^-	254	120	8	800	625
KBr:SH^-	332	120	8	800	625
KI:Ag^+	17.3	91	7.7	60	34

For higher temperatures, γ_A is obtained by extrapolating these experimental data.

With the above parameters, the absorption spectrum is plotted in Fig. 3(a) for three temperatures. The strength of the resonant mode decreases rapidly with increasing temperature in agreement with experiment [13]. At low temperatures, the decrease in the resonant mode strength follows the change in the on-center population. At higher temperatures the Ag^+ ion jumps so rapidly from one configuration to the other that no evidence of the resonant mode remains (cf. the dashed curve). To compare directly with the experimental strengths, the calculated absorption spectra are integrated from 10 to 25 cm^{-1} and the nearly flat Debye contributions over this same region are subtracted off (in the same way that the experimental data were analyzed). Results are normalized to the zero-temperature strength and plotted in Fig. 3(b) as the solid curve. Excellent agreement is obtained with experiment graphed by the filled circles. Similar analysis of the temperature-dependent strengths of the pocket gap modes [6] using the same parameters also agrees with experiment [13].

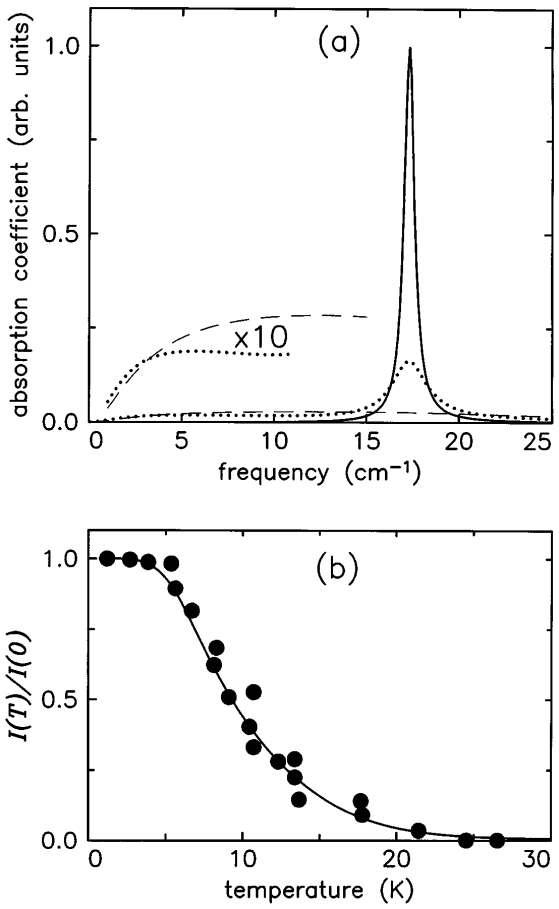

FIG. 3. (a) Impurity-induced FIR absorption spectra of KI:Ag^+ calculated from Eq. (6) using the parameters given in Table I. The temperatures are 1.2 K (solid curve), 10 K (dotted curve), and 22 K (dashed curve). The high temperature curves have also been plotted with 10-fold vertical expansion at low frequencies to show the Debye peaks. (b) Absorption strengths of the KI:Ag^+ resonant mode normalized to the lowest temperature. The solid curve is calculated according to the procedure described in the text and the filled circles are experimental data from Ref. [13].

In summary, we have analyzed the unusual temperature-dependent behavior of the librational modes of diatomic chalcogen hydrides in fcc alkali halides and the resonant mode of KI:Ag^+ in terms of two different defect configurations which coexist at low temperature but which are separated from each other by a large potential barrier. In both cases, our generalized jump-rotational-diffusion model successfully accounts for the temperature dependences of the IR absorption spectra. Hence, the identification of harmonic librational or vibrational modes for a particular elastic configuration of a defect system does not exclude the possibility that at some other temperatures the system may exhibit two-state dynamical behavior.

We thank J. B. Page and R. H. Silsbee for many helpful discussions. Work supported by NSF-DMR-9312381 and ARO-DAAL03-92-G-0369. Use was made of the MRL central facilities supported by NSF-DMR-9121654.

*Present address: Los Alamos National Laboratory, Mailstop E548, Los Alamos, NM 87545.

[1] D. B. Fitchen, in *Physics of Color Centers*, edited by W. B. Fowler (Academic Press, New York, 1968), p. 318.
[2] H. Bilz, D. Strauch, and R. K. Wehner, in *Encyclopedia of Physics*, edited by L. Genzel (Springer, Berlin, 1984), Vol. XXV/2d, p. 420.
[3] J. B. Page *et al.*, Phys. Rev. Lett. **63**, 1837 (1989).
[4] F. Bridges and M. Jost, Phys. Rev. B **38**, 12 105 (1988).
[5] C. E. Mungan, U. Happek, and A. J. Sievers, J. Lumin. **58**, 33 (1994).
[6] K. W. Sandusky *et al.*, Europhys. Lett. **27**, 401 (1994).
[7] K. S. Singwi and A. Sjölander, Phys. Rev. **119**, 863 (1960).
[8] K. E. Larsson, J. Chem. Phys. **59**, 4612 (1973).
[9] K. Lindenberg and R. I. Cukier, J. Chem. Phys. **62**, 3271 (1975).
[10] B. K. P. Scaife, *Principles of Dielectrics* (Clarendon Press, Oxford, 1989), p. 350.
[11] J. McConnell, *Rotational Brownian Motion and Dielectric Theory* (Academic Press, London, 1980), p. 36.
[12] H. Fröhlich, *Theory of Dielectrics* (Clarendon Press, Oxford, 1958), 2nd ed., p. 68.
[13] A. J. Sievers and L. H. Greene, Phys. Rev. Lett. **52**, 1234 (1984).
[14] A technical point is that the on-center state (A) of KI:Ag^+ has no permanent dipole moment, while Eq. (6) incorporates a small rf contribution from such a feature. This would appear in RbCl:Ag^+ but must be subtracted off here.
[15] S. B. Hearon and A. J. Sievers, Phys. Rev. B **30**, 4853 (1984).
[16] L. H. Greene, Ph.D. thesis, Cornell University, 1984.